SSRG International Journal of Electrical and Electronics Engineering
ISSN: 2348-8379/ https://doi.org/10.14445/23488379/IJEEE-V13I2P101

Volume 13 Issue 2, 1-14, February 2026
© 2026 Seventh Sense Research Group®

Original Article

Metaheuristic Tuning of Cascade PI Controller for DC Machine Speed Control in Meca-Electrical Wind Pumping Systems using Genetic Algorithm and Hybrid ACO-PSO Optimization

Abdelkader ELMEDDAH[1,2], Djalloul ACHOUR[1,3]

[1]*Department of electronics, Faculty of Technology, Hassiba Benbouali University, Chlef, Algeria.*
[2]*Laboratory of Electrical Engineering and Renewable Energies, Chlef, Algeria.*
[3]*Laboratory of Applied Automation, Boumerdes, Algeria*.

[1]*Corresponding Author : a.elmeddah@univ-chlef.dz*

Received: 11 November 2025 Revised: 16 December 2025 Accepted: 12 January 2026 Published: 17 February 2026

Abstract *- Hybrid water pumping systems have increasingly been recognized as a reliable and sustainable alternative for supplying water in isolated areas. These kinds of systems harness natural energy sources, more significantly wind and solar, to guarantee that water is always there, without depending on traditional power lines. Among the different setups, the Meca-Electrical Wind Pumping System has been the subject of much research because of its capacity to incorporate both mechanical and electrical wind pumping systems' advantages. The functioning of the system is mainly based on the DC machine, which is controlled by a bidirectional DC-DC converter. For keeping the system in a stable operation, usually, a PID controller is employed because of its simple structure and easy design. But the usual PI control does not often do a good job of coping with the nonlinearities and complex dynamics of the system. To tackle these issues, a cascade PI controller is proposed, which brings in a dual-loop control system that boosts the accuracy and speed of responses. The best adjustment of controller settings is done with the help of modern optimization techniques, mainly the Genetic Algorithm (GA) and a hybrid Ant Colony Optimization and Particle Swarm Optimization (ACO-PSO). The simulation results that were obtained in simpowersystem MATLAB/Simulink show that both strategies lead to a notable enhancement in the stability and performance of the system, with ACO&PSO being the one that exhibits the best tuning capability and dynamic response.*

Keywords *- Five Cascade PI Controller, DC machine, Bidirectional DC-DC Converter, Genetic Algorithm (GA), ACO-PSO algorithm.*

1. Introduction

Access to clean water is still one of the most primary problems in rural and isolated areas, and the absence of electrical infrastructure hinders the installation of traditional pumping systems [1, 2]. Renewable energy technologies are getting a lot of attention. They are used as clean and sustainable ways to pump water [3]. The energy of wind is one of the main renewable energy sources. It is easily obtainable, so it does not have a big environmental footprint, and it drastically reduces the use of fossil fuels [4]. One of the earliest forms of wind energy utilization to achieve water movement is the mechanical wind pumping systems, especially in rural off-grid locations. The performance of these systems is acutely dependent on variations in wind speed, and the accompanying absence of energy storage or even complex control strategies is a major hiccup in the capacity to provide a unvarying and continuous water supply [5]. The electrical wind pumping systems change the wind energy into electrical energy, which is easier to manipulate, provides operational flexibility, and allows for the addition of energy storage devices. These characteristics allow a more controlled pump operation process in changing wind conditions. However, this requirement of power electronic converters and control units adds complexity, costs, and conversion losses to the system over just mechanical solutions [6].

To address the constraints of both mechanical and electrical designs, the Mecha-Electrical Wind Pumping System (MEWPS) has been developed to achieve the strength of mechanical and flexibility and controllability of electrical systems. In these systems, the DC machine is very important. This is the device that changes the wind energy into mechanical energy for the pump. On the other hand, it is difficult to keep its speed constant most of the time since the


This is an open access article under the CC BY-NC-ND license (http://creativecommons.org/licenses/by-nc-nd/4.0/)

wind power and the load vary. Moreover, if no speed regulation is in place, the system can become unstable, the efficiency of pumping will be lower, and the machine may have a shorter lifespan due to more stress. Hence, it is very important to utilize powerful control techniques to maintain the speed of the DC machine within the required limits and thus ensure the smooth operation of MEWPS.

The speed of separately excited DC machines has always been controlled by simple linear controllers, where such controller solutions as the Proportional-Integral (PI) type were usually selected as the best ones [7].

The main reason for the wide acceptance of PI controllers is their ease of realization, low price, and the fact that they can provide a good performance in a number of different applications [8].

However, traditional PI controllers are usually found to be insufficient when implemented in nonlinear systems like MEWPS having time-varying dynamics. Among the limitations are significantly low tracking precision, overshoot, and prolonged settling times in the case of disturbances.

The boundaries of the traditional PI controllers in intricate systems frustrated the engineers. The researchers were trying to come up with a better way, and one of the proposed methods, the cascaded PI controller, started drawing attention [9].

A two-tiered approach to the PI controller is applied in this arrangement. One loop does the inner loop control, and the other one oversees the outer loop. The improved disturbance rejection and the more flexible tuning process result from this setup [10]. However, the primary issue is still the determination of appropriate values for the controller gains, as they have a very strong influence on the stability and performance of the system.

Traditional tuning of control loops (such as using Ziegler-Nichols rules, trial and error adjusting...) frequently fails with complicated systems. Such techniques typically assume that the system is linear and can give results that are far from optimal if the system is nonlinear, its parameters change, or there are some disturbances [11]. Evolutionary optimization methods have been employed in the controller design stage to eliminate these deficiencies.

These algorithms, inspired by natural or social processes, provide global optimization capabilities and are able to solve different hard engineering problems [12]. Genetic Algorithm (GA) comes from biological evolution [18]. GA improves the quality of solutions by means of various operators like crossover, mutation, and selection. Given its strong and globally searching nature, GA has been widely used for PI tuning [13]. Particle Swarm Optimization (PSO) mimics the behavior of birds or fish when they move or travel together [14]. With PSO, particles are able to communicate information, and they can quickly come together to find the best solutions [15]. Ant Colony Optimization (ACO) is based on the way that the ants find food. ACO is good at exploring and not getting stuck in local minima. However, it can have a problem with slow convergence [16, 17].

The main problem with the previous research is that it was mostly concentrated on the conversion of power and offered no realistic dynamical representation of the system.

A detailed dynamic model of MEWPS was created in this work, comprising a separately excited DC machine, the bidirectional DC-DC converter, and the battery bank. This paper has helped advance the current study on wind energy-based pumping systems by:

- The design of a cascaded PI controller to regulate the speed of a DC machine in MEWPS.
- Tuning the parameters of the controllers in MEWPS through application of two optimization methods, Genetic Algorithm (GA) and hybrid ACO and PSO.
- Conducting a comparative analysis in terms of convergence of cost functions, development of PI parameters, and classical performance indexes (IAE, ISE, ITAE, overshoot, and steady-state error).
- Testing the soundness of the suggested strategies in two dynamic conditions, constant the speed of reference and variable load torque, and constant load torque and variable reference speed.

2. Electrical Subsystem Modeling

The electrical part of the MEWPS is mainly about the bidirectional DC-DC converter, the DC machine, and the battery bank.

The DC machine in this setup can transfer excess energy generated by the wind turbine via the DC-DC converter to the battery bank for charging. Later, this energy can be used when the wind turbine is not available for water pumping, as shown in Figure 1.

2.1. DC Machine Model

The modeling of the DC machine relies on the description of the machine changes, both on the electrical and mechanical sides.

In this set of equations, the field winding is fed from a separate DC source; thus, the magnetic flux remains constant.

The armature (rotor) circuit is the one characterized by the voltage equation, which includes terms for the applied voltage, armature resistance, and inductance, and also the Electromotive Force (EMF) generated by the rotor.

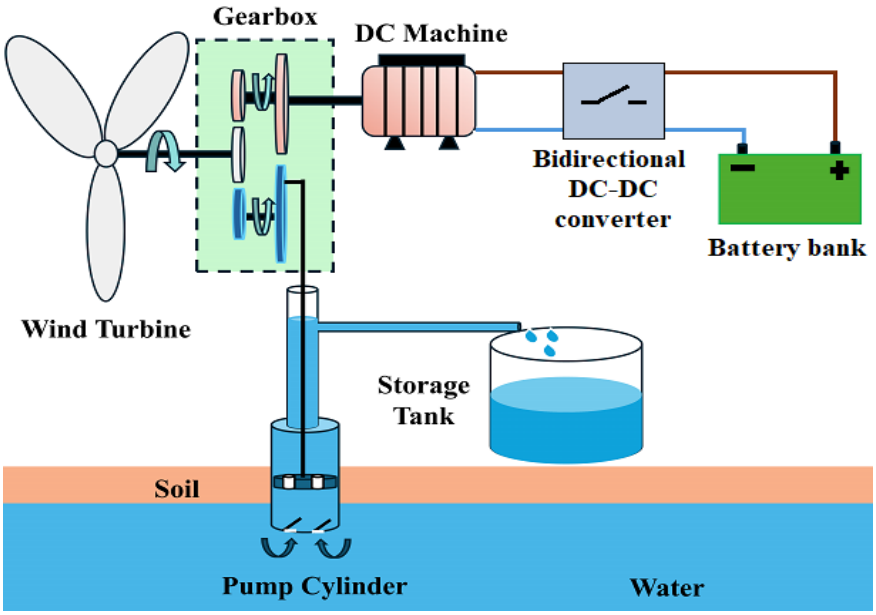

Fig. 1 Meca-electrical wind pumping system

The load, thus, is driven by the electromagnetic torque, which is balanced by the inertia and friction of the machine [18]. The mathematical model is described by the following equations:

- Armature voltage equation

$$V_a(t) = R_a \cdot i_a(t) + L_a \cdot \frac{di_a(t)}{dt} + e_b(t) \quad (1)$$

Where: V_a is the armature voltage (V), R_a the armature resistor (Ω), i_a the armature current (A), L_a the armature inductance (H), e_b EMF voltage (V).

- EMF relation

$$e_b(t) = K_e \cdot \omega(t) \quad (2)$$

Where: K_e is the voltage constant, and ω is the machine speed (rad/s)

- Electromagnetic torque equation

$$T_e(t) = K_t \cdot i_a(t) \quad (3)$$

Where: K_t is the torque constant.

- Mechanical dynamics

$$j\frac{d\omega(t)}{dt} = T_e(t) - T_L(t) - B_m\omega(t) - T_f(t) \quad (4)$$

Where: T_e is the electrical torque (N.m), T_L is the load torque (N.m), J is the inertia (Kg.m^2), B_m is the viscous friction coefficient, T_f is the coulomb friction torque (N.m).

The parameters of the separately excited DC machine are identified and presented in Figure 2.

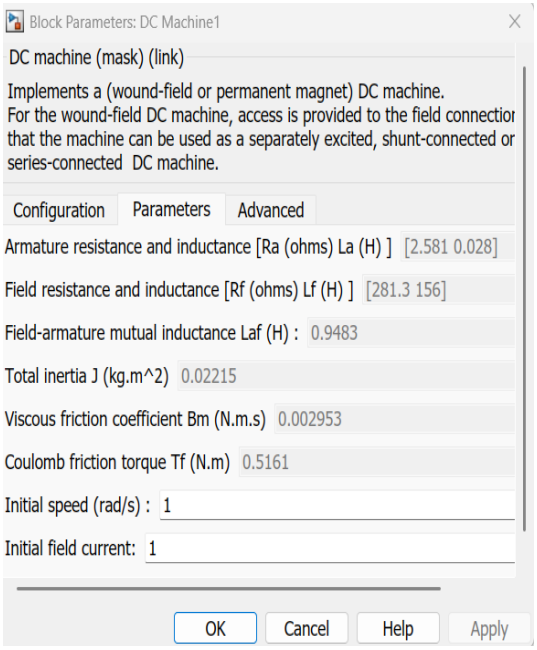

Fig. 2 Separately excited DC machine settings

2.2. Bidirectional Buck-Boost Converter

It is the main unit for energy management. This converter allows the battery to be charged and discharged [19].

2.2.1. Charging Mode

By utilizing this mode, the converter operates as a buck DC converter; thus, the additional energy from the DC generator is forwarded to the battery. The charging of the battery is made more efficient with the help of the duty cycle that regulates the output voltage and, at the same time, prevents overvoltage [20]. The output voltage is expressed as:

$$V_{battery} = D \cdot V_{DCmachine} \quad (5)$$

Where: $V_{battery}$ is the battery voltage (V), and $V_{DCmachine}$ is the DC machine voltage (V).

2.2.2. Discharging Mode

When the power of the wind turbine is not enough, the converter works as a boost converter, taking energy from the battery to feed the DC machine. The duty cycle regulates the voltage; thus, the operation of the machine is good, and the battery is safe from a deep discharge. The output voltage is given by:

$$V_{DCmachine} = \frac{D}{1-D} V_{battery} \quad (6)$$

Table 1 determines the parameters of this converter.

Table 1. Parameters of bidirectional DC-DC converter

Parameters	Values
Switching frequency (Sf)	10000 Hz
Duty cycle (D)	0 to 0.95
Inductor (L)	1.247×10^{-3} H
Capacitor (C)	0.003565 F
Bus Capacitor (C_{bus})	0.001 F

2.2.3. Battery Bank Model

The battery in MEWPS stores extra energy during high wind and supplies it during low wind. Its behavior is modeled by a simple dynamic model that links state of charge (SOC), current, and terminal voltage. Its behavior can be represented by a dynamic model, expressed as:

$$V_{\text{battery}}(t) = V_{oc} - R_{int} \cdot i_{\text{battery}}(t) \quad (7)$$

$$SOC(t) = SOC(0) - \frac{1}{C_{\text{battery}}} \int i_{\text{battery}}(t)\, dt \quad (8)$$

Where: V_{oc} is the open-circuit voltage of the battery (V), R_{int} is the internal resistance of the battery (Ω), $i_{battery}$ is the battery current, *SOC* is the state of charge of the battery, and $C_{battery}$ is the battery capacity (Ah).

The battery parameters are determined in Figure 3.

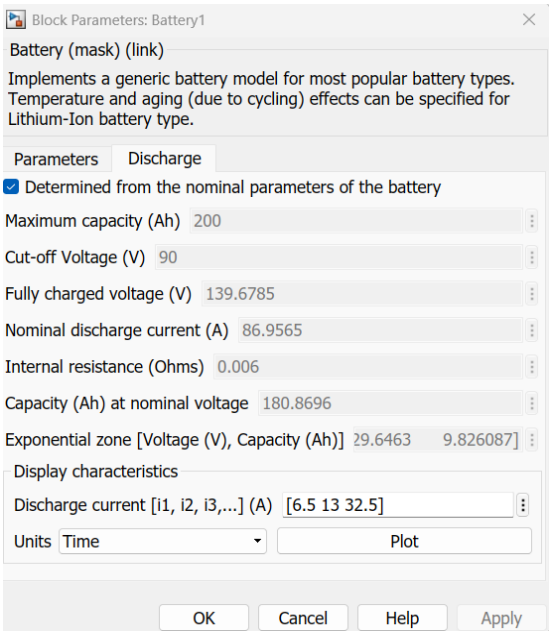

Fig. 3 Settings of battery bank

3. Cascade PI Controller Design

The cascade PI controller incorporates two loops that are coupled to maintain the system steady. The PI controller uses the desired armature voltage in an outer loop and the actual voltage of the DC machine. It then drives a current reference even to the inner loop. The inner loop responds quickly to ensure that the current of the battery is in a way that it conforms to this reference, which assists the system in responding immediately to the disturbances. Through the coordination of the two loops, the DC machine is in a position to maintain a constant speed even when the load or the required DC machine speed varies, as seen in Figure 4.

3.1. Optimization Technique

The cascade PI controller should be tuned to get good results. Complex nonlinear systems such as MEWPS do not usually react well to old methods such as trial-and-error, root locus, or pole placement. Conversely, bio-inspired optimization techniques have the ability to automatically find the optimal gain values, making their use more effective and less prone to error.

3.1.1. Genetic Algorithm (GA)

Biological evaluation is the source of inspiration for the GA. In PI controller tuning, every person in the population is a potential parameter set (K_{P1}, K_{I1}, K_{P2}, K_{I2}).

GA also uses selection, crossover, and mutation to evolve a population through generations and efficiently search for the best parameter values of the PI controller [21].

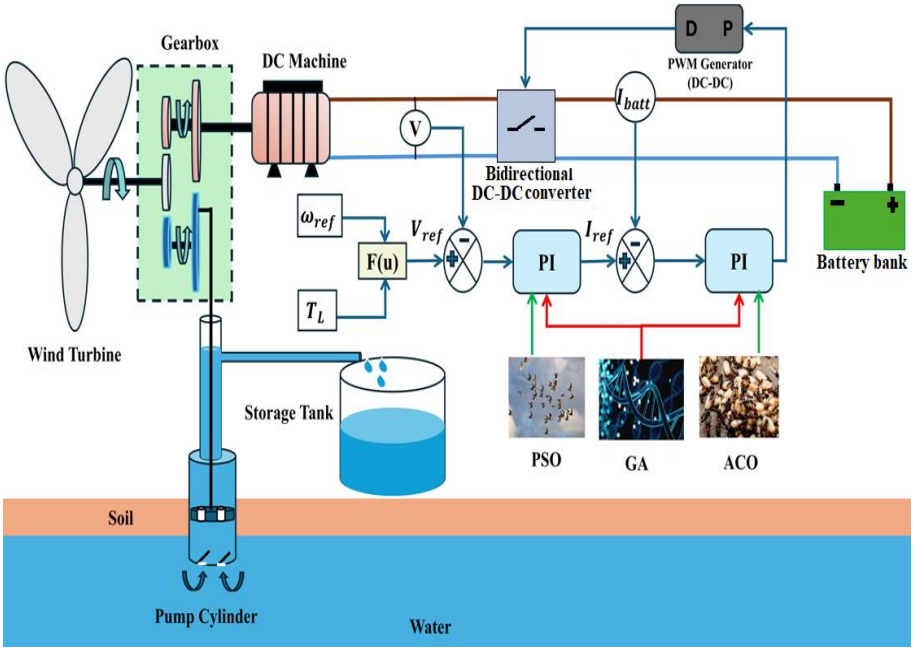

Fig. 4 Cascade PI controller strategy for controlling the DC machine speed

Particle Swarm Optimization (PSO)

The PSO algorithm is based on the movement of traveling birds and fish. In the PI controller tuning, all the particles of the swarm are candidate solutions that are characterized by the outer loop parameters (K_{P1}, K_{I1}). Swarm members share information on the best positions that they are in, and then modify their search space movements to enable the swarm to converge on the best values [22].

Ant Colony Optimization (ACO)

The ACO algorithm is based on the foraging activity of ants and their pheromone trails. With PI controller tuning, an ant constructs a potential solution with the parameter values of inner loops (K_{P2}, K_{I2}). In the course of time, more powerful pheromone trails direct other ants to more appropriate solutions, balancing between exploration and exploitation during the search process [23]. Tuning cascade PI controllers in MEWPS using GA and ACO-PSO is better than the traditional means. GA offers a global search that does not suffer from local minima and is effective in nonlinear dynamics, whereas hybrid ACO-PSO achieves great exploration with rapid convergence.

Configuration of Optimization Methods for Cascade PI

The optimization setup explains how the cascade PI controllers are tuned. It defines the decision variables, the cost function, the constraints, and the steps to follow when running the GA and ACO-PSO algorithms.

Decision Variables

The cascade PI structure has four parameters. The PI gains of the current loop (K_{P2}, K_{I2}) and the voltage loop (K_{P1}, K_{I1}). These parameters are chosen carefully to keep the system stable and to give flexibility for improving performance.

Cost Function

The cascade PI controller in the MEWPS is tuned by minimizing the cost function Jcost, which measures system performance. The PI parameters (K_{P1}, K_{I1}, K_{P2}, K_{I2}) are tested in the Simulink model.

The voltage, current, and speed responses are then compared with their reference signals. The cost function is calculated as a weighted Integral of Absolute Errors (IAE).

$$J_{cost} = \alpha \int_0^T |e_V(t)|\,dt + \beta \int_0^T |e_I(t)|\,dt + \gamma \int_0^T |e_S(t)|\,dt \quad (9)$$

Where: e_V is the voltage error, e_I is the current error, and e_S is the speed error; α=0.4, β=0.3, and γ=0.3 are weighting factors.

Minimizing J_{cost} improved response time, reduced error, and augmented robustness under the nonlinear and time-varying dynamics of the MEWPS.

Constraints

Practical limits are applied to the PI gains to keep the system stable. These limits also define the search space for the GA and ACO-PSO algorithms. This helps the algorithms find optimal and physically meaningful controller parameters. The parameters are given as follows:

$$\begin{cases} 0 \le K_{P1} \le 50 \\ 0 \le K_{I1} \le 50 \\ 0 \le K_{P2} \le 50 \\ 0 \le K_{I2} \le 50 \end{cases} \quad (10)$$

Flowchart

The GA tunes all cascade PI parameters at once, as shown in Figure 5.

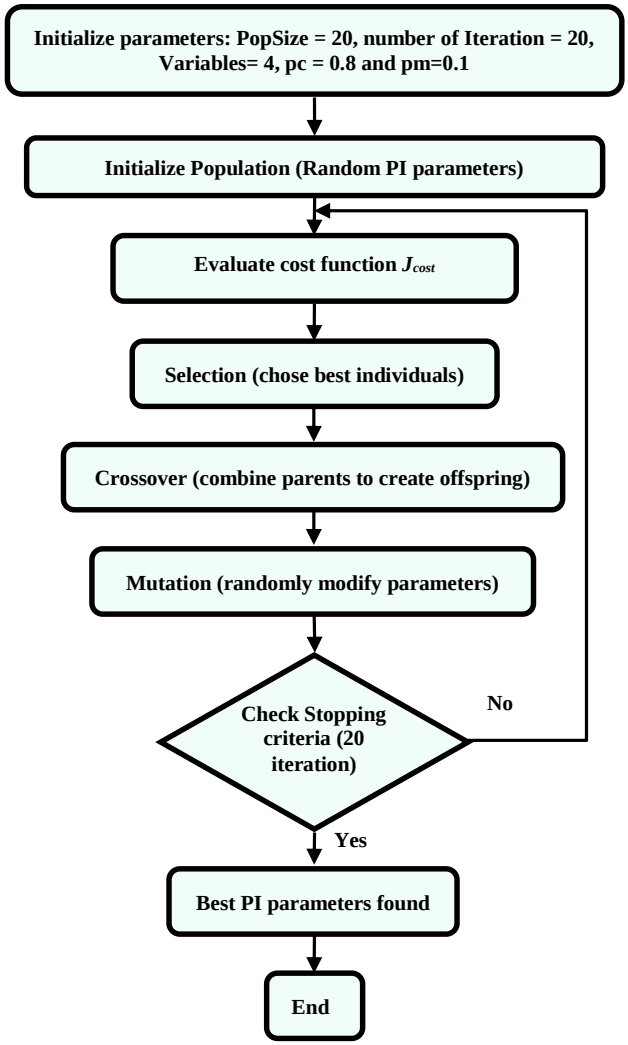

Fig. 5 Flowchart of the GA algorithm

On the other hand, ACO-PSO tunes the cascade PI in parallel. PSO adjusts the outer voltage loop, while ACO is adjusted to the inner current loop. The tuning steps are illustrated in Figure 6.

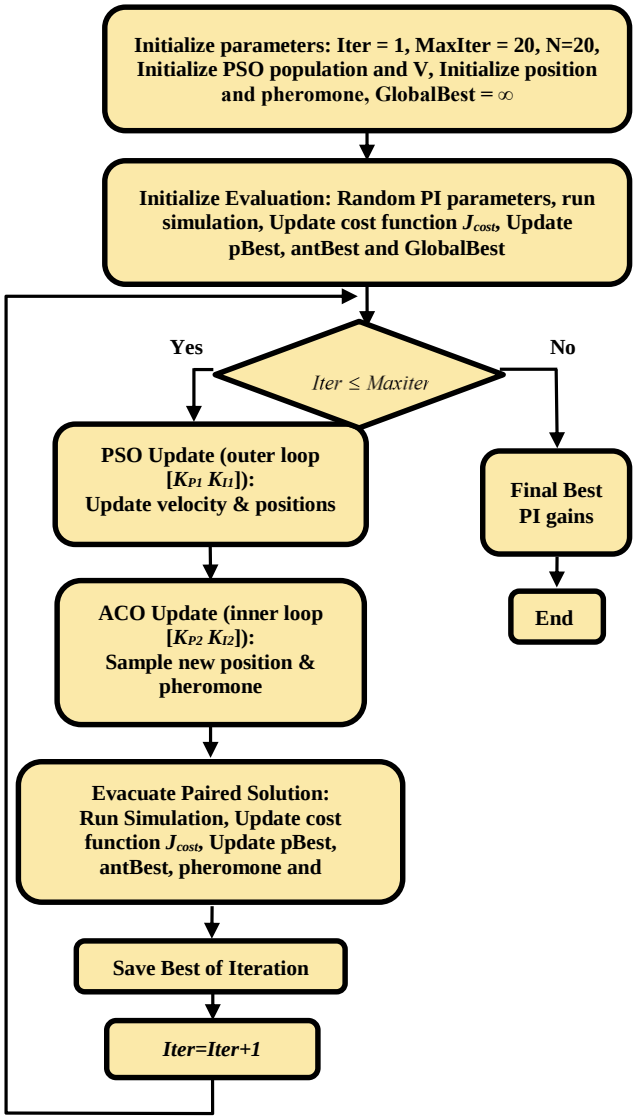

Fig. 6 Flowchart of ACO-PSO algorithm

4. Simulation Results and Discussion

The simulation results are powered by SimPowerSystems MATLAB/Simulink, and the results are divided into two parts. First, a comparison between the GA and ACO-PSO algorithms is presented for tuning the PI parameters. Then, the dynamic behavior of the DC machine speed, battery current, and armature voltage is analyzed under two operating scenarios: fluctuating load torque at a fixed speed and fluctuating speed at a fixed load torque.

4.1. Performance Comparison of the Algorithms

The fact that the cost function has come to a convergence point, as represented in Figure 7, was clear evidence of a clear difference in the convergence of the optimization process between the Genetic Algorithm (GA) and the hybrid ACO-PSO optimization strategy. Concerning the GA, the cost model was initially started at 11.65 and showed a slight decline to 11.575 at the third run, then remained almost the

same until the fifteenth run. After that, it slightly decreased to 11.55, which was a figure that remained constant during the twentieth iteration. The trend is a sign of premature convergence, in which GA quickly monetized its original solutions but could not achieve any more substantive gains. On the other hand, the hybrid ACO-PSO started with a lower starting value of 10.65, which it maintained until the sixth iteration. Since the eighth time, the cost function has fallen to 10.50 and has not changed since then until the end of the experiment.

This result indicates that the hybrid methodology not only provides better initial solutions but also provides a successful balance between exploration and exploitation, thus avoiding local solutions and converging towards a more precise solution. Subsequently, the findings support the fact that ACO-PSO was better than GA in convergence rate, final stability, and quality of the overall solution to tuning of the cascaded PI controller in magnetically enhanced wound field power supply (MEWPS) applications.

The convergence analysis of the PI controller parameters, in Figure 7, clearly shows differences between the GA and the hybrid ACO-PSO algorithm. In the case of K_{P1}, GA was basically the same value at all iterations, approximately 4.7404, so it reached a premature stagnation; however, ACO-PSO started at 1.0 and progressively increased until it reached 1.1922 at the 6th iteration, therefore, showing an adaptive smoother convergence trajectory. In the case of K_{I1}, the value of GA decreased significantly by iteration 4 to 5.6888, and then the value remained constant, whilst ACO-PSO started with 42, rose to 50 at iteration 6, and remained highly adaptable after that. In the case of K_{I2}, GA showed a steep decline between 30 and 6.5974 at iteration 3, indicating a quick but unsteady adaptation of the process.

Concurrently, ACO-PSO took a dynamic curve, beginning with a value of 4, iterating to 50, and stabilizing with a solid value of 3.0228 after iteration 9. The curve shows its exploration ability before converging. Lastly, in regard to K_{P2}, GA began with a value of 46, dropped to 14 at iteration 3, leveled out until iteration 10, and continued to rise to 34.927, whereas ACO-PSO began with 19, peaked to 38 at iteration 6, dropped to 16, and peaked again at 45.927 at iteration 17, indicating a lack of consistency. The above observations support the fact that GA is preterm and rigid in contrast to ACO-PSO, which has a more balanced exploration and exploitation paradigm, leading to high-quality and more vigorous PI parameter optimization.

The performance indices that have been identified under Table 2 highlight the differences between the Genetic Algorithm (GA) and hybrid Ant Colony Optimization-Particle Swarm Optimization (ACO-PSO) methods in tuning a cascaded Proportional-Integral (PI) controller. Regarding parameter selection, GA was closer to comparatively higher values of, e.g., K_{P1} (4.7404) and K_{I2} (6.5974), whereas the ACO-PSO method was much more balanced with, e.g., K_{I1} (50) and K_{P2} (45.927) being much larger, consequently, suggesting a higher adaptability. As far as error indices are concerned, the ACO-PSO approach was always better than the GA approach, where the Integrated Absolute Error (8.639 versus 10.338), Integrated Squared Error (712.97 versus 774.07), and Integrated Time-Weighted Absolute Error (0.45175 versus 0.80026) are lower. These cutbacks represent an improvement in accuracy and faster error compensation. With respect to the transient response, the GA had a minor negative overshoot of (-0.21), which indicates a slightly conservative response, and the response of ACO-PSO had a moderate positive overshoot of 2.77, which reflects a more dynamic response but within acceptable stability limits.

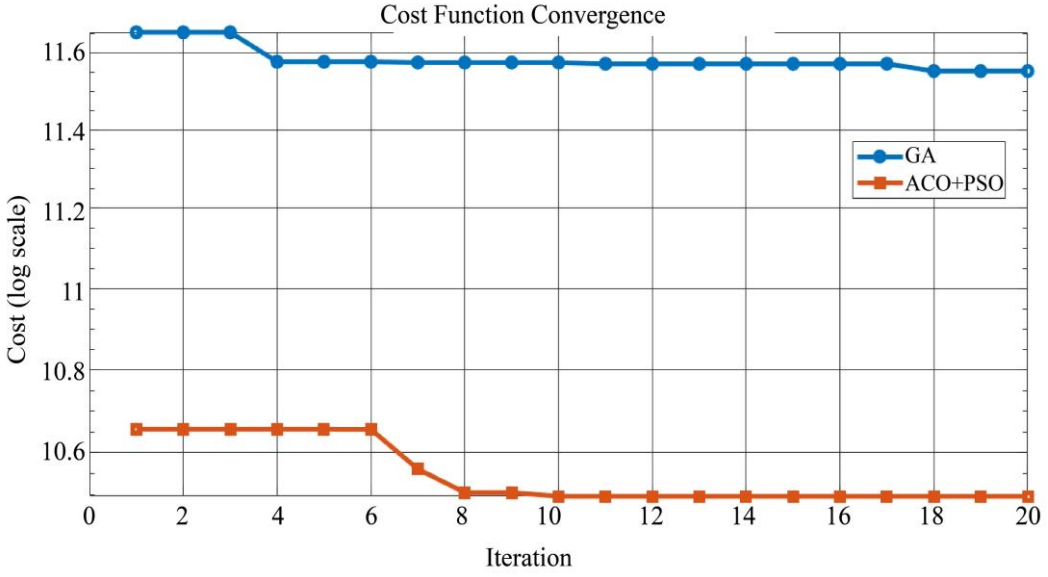

Fig. 7 Cost function convergence

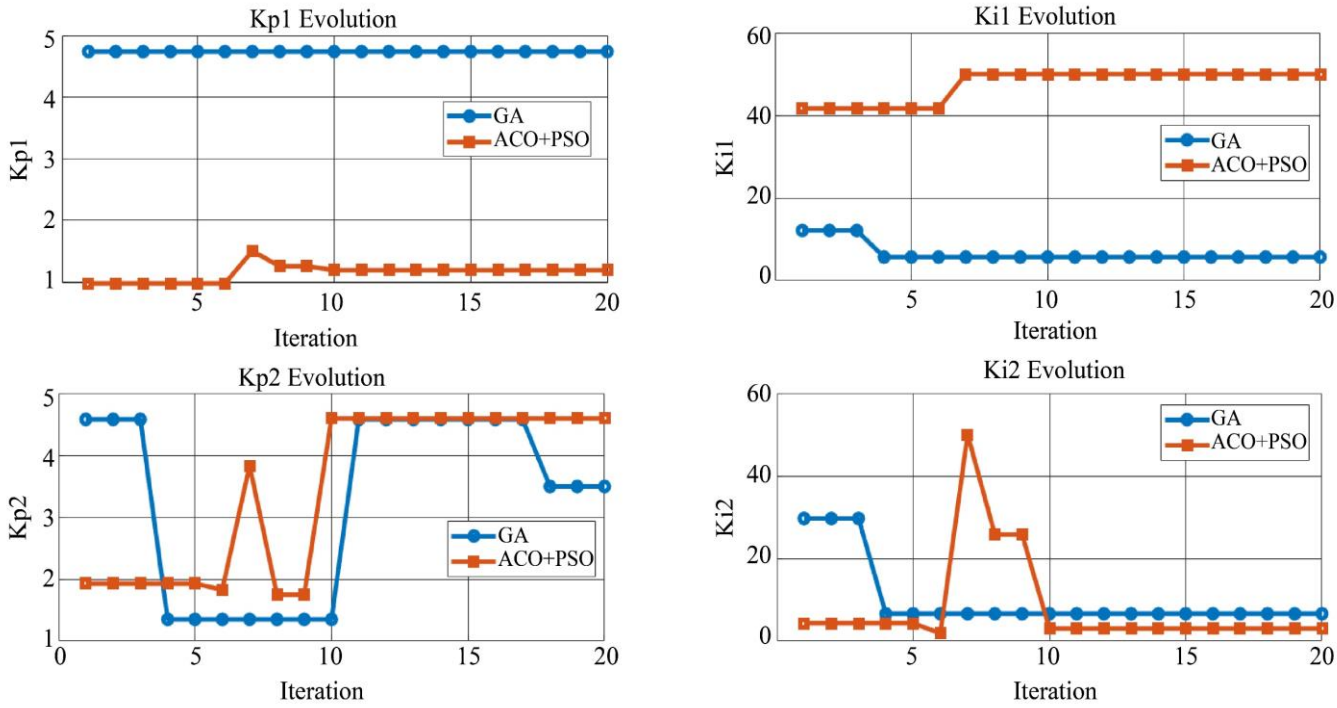

Fig. 8 PI parameters convergence

In terms of steady-state performance, considering the reference speed at 130 0 rad/s, the ACO-PSO recorded a steady-state performance of 129.99 0 rad/s, which is very close to the target, unlike the GA, which had 129.71 0 rad/s. This observation attests to the fact that the ACO-PSO, in addition to minimizing dynamical and integral error, also provided better steady-state tracking. Overall, the GA provided conservative tuning with little overshoot, greater errors, and decreased steady-state accuracy. The hybrid ACO-PSO, in its turn, achieved a more desirable compromise between error reduction, temporary dynamics, and steady-state fidelity, becoming the more effective optimization method to be used in cascaded PI controller design in MEWPS applications.

Table. 2 Performance comparison between GA and ACO&PSO algorithm

Algorithm	K_{P1}	K_{I1}	K_{P2}	K_{I2}	IAE	ISE	ITAE	Overshoot	Steady State
GA	4.7404	5.6888	34.941	6.5974	10.338	774.07	0.80029	-0.21115	129.71
ACO-PSO	1.1922	50	45.927	3.0228	8.639	712.97	0.45175	2.7746	129.99

4.2. Dynamic Behavior of DC Machine Speed, Battery Current, and Armature Voltage

This part discusses the dynamic behavior of speed, current in the battery, and armature voltage of a DC machine. The functionality of the performance is evaluated in different conditions of operation in order to show how the system will react to the change in the load torque and the speed of the system.

Test 1: Constant Speed and Variable Load

The values of DC machine load torque are presented in two modes: motor and generator, as shown in Figure 9. In this test, the machine operated at 135 rad/s in motor mode and 175 rad/s in generator mode.

As shown in Figure 10, both GA and ACO-PSO could trace the reference speed, though ACO-PSO attained significantly higher velocity and accuracy. ACO-PSO reached the desired speed sooner in motor mode (130rad/s) and resumed after being disturbed in 0.2s, as compared to GA, which took about 1s.

Under generator mode (170 rad/s), ACO-PSO settled quickly with a low overshoot, but GA had a large settling point and a longer settling time. In general, ACO-PSO had better tracking fidelity, faster disturbance rejection, and higher stability, which corroborates the fact that it is more reliable when used in the actual operation of MEWPS. The dynamic current response in Figure 11 shows that the proposed cascaded PI control strategy is effective in controlling the current according to the changes in load torque.

The charging current at the generator mode or the discharging current at the motor mode increases with the load

torque, hence maintaining a healthy work of the system. The controller of GA based, however, has a strong performance in terms of ripples and oscillations compared to a smooth performance when using the ACO-PSO controller. Such ripples highlight the small amount of strength of the GA and may even destroy the battery and the bidirectional DC-DC converter.

On the other hand, the current profile of the ACO-PSO methodology is more balanced and damped, and the oscillations quickly dissipate after disruptions.

This comparative analysis shows that the hybrid algorithm is a better balance between a fast response and stability, therefore, improving a higher degree of reliability and increasing the life cycle of the energy storage system and power electronic parts. As shown by the dynamic voltage response in Figure 12, armature voltage increases proportionately to an increase in load torque during both motor and generator configurations and vice versa.

This observation is in line with the direct proportionality between torque and voltage in DC machines. The ACO-PSO controller considerably suppresses voltage oscillations in either of the operating modes compared to the GA controller. Besides, in the switching of the motor into the generator mode, the ACO-PSO controller reaches the reference voltage in a shorter time, with its response being much faster, in contrast to the GA controller, which has a pronounced overshoot and long settling time.

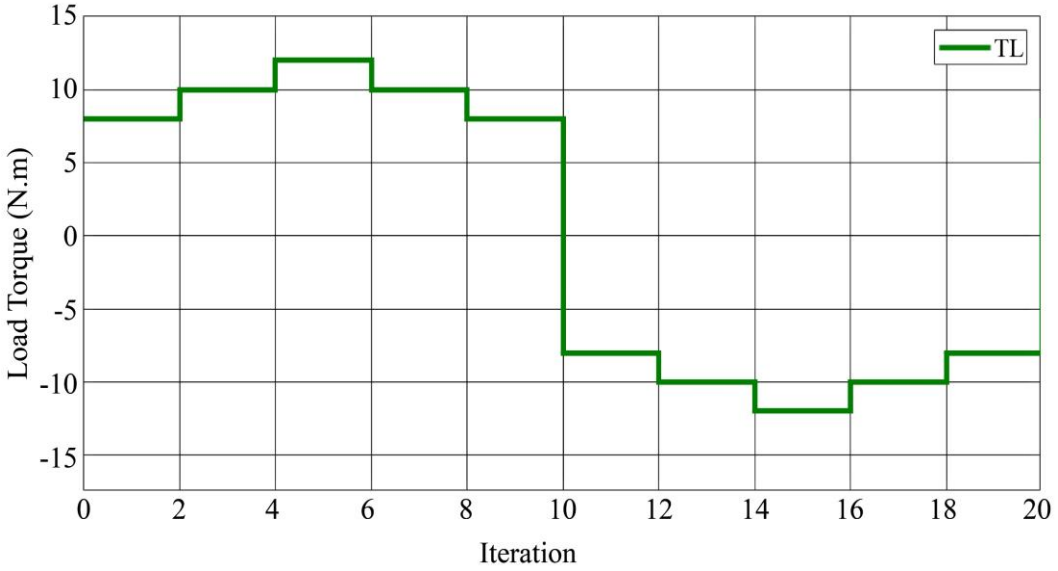

Fig. 9 Load torque variation

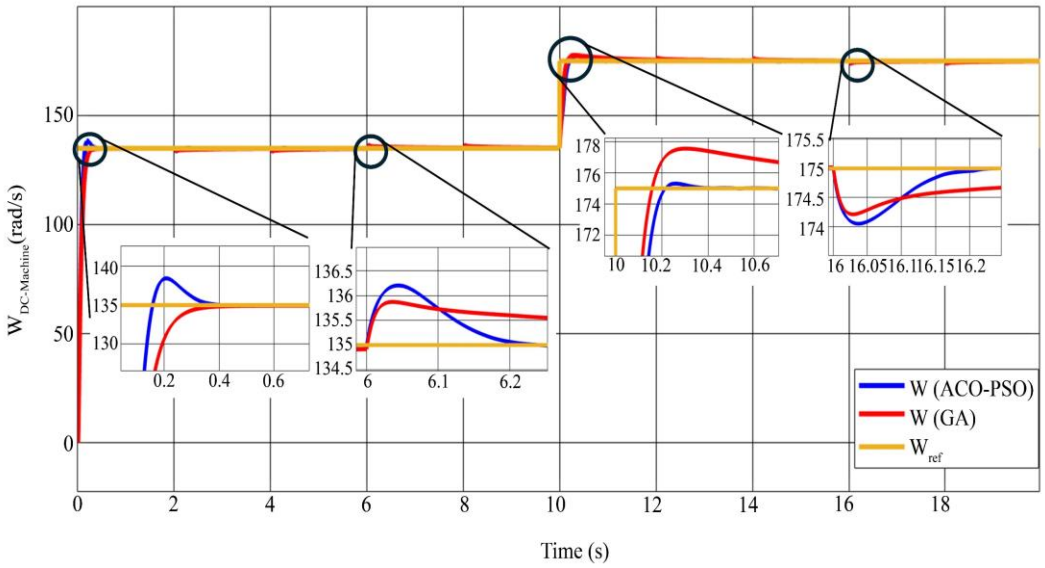

Fig. 10 Dynamic DC machine speed

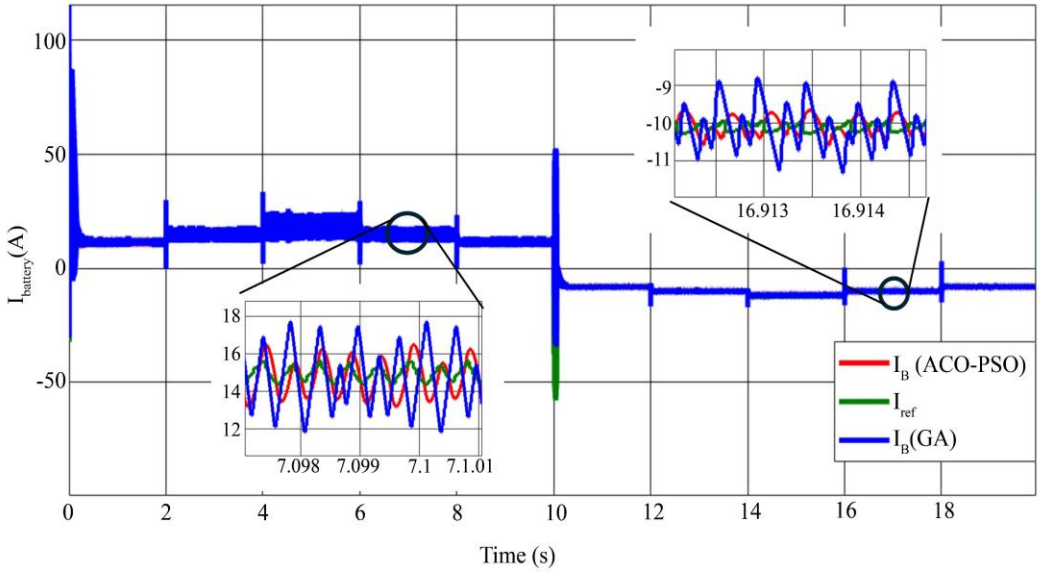

Fig. 11 Dynamic battery current

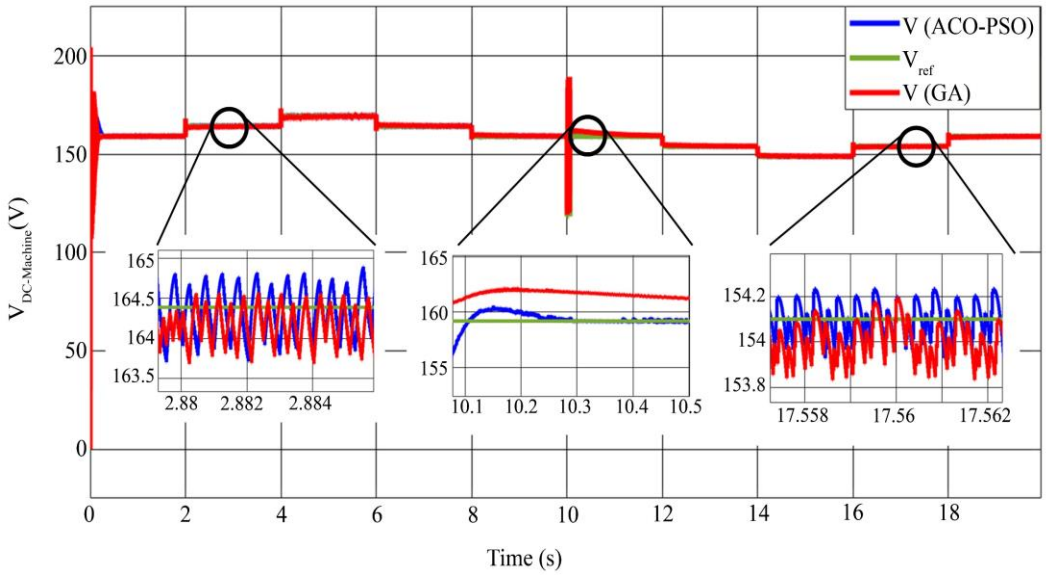

Fig. 12 Dynamic armature voltage

Test 2: Variable Speed and Constant Load

In this scenario, the DC machine load torque was kept constant at (10 N.m) in motor mode and (-10 N.m) in generator mode, as shown in Figure 13. Meanwhile, the DC machine speed was varied, as illustrated in Figure 14.

The dynamic speed of the DC machine was illustrated in Figure 14, where the load torque had been kept constant, and the reference speed had been varied; the results had revealed clear differences between the two algorithms. The ACO-PSO controller had exhibited a relatively large overshoot at the beginning, but its response had been significantly faster compared to GA. When the reference speed was varied, ACO-PSO could rapidly trail and update its value, whereas GA took a longer time to adapt. At this motor-to-generator switchover, GA had exhibited high overshoot and required approximately 3 seconds to stabilize, whereas that required for the ACO-PSO system was only about 0.5 seconds. ACO-PSO also obtained sufficient and useful information about the new reference with respect to generator mode operation (under these new reference speeds), and its performance remained stable while GA was unable to deal with the change. These had to establish that ACO-PSO had provided better dynamic speed response, quicker adaptation to speed changes, and a more observable behavior in starting mode-change than the GA. The dynamic behavior of the battery current is represented in Figure 15. This behavior has been shown to be directly related to the reference speed. For high speeds, battery current increases, while for low speeds, a decrease in current has been observed. Current was controlled by both algorithms,

but GA showed significantly more oscillations compared to ACO-PSO. The presence of these oscillations implies that the current regulation by GA was less reliable and could have had an unfavorable impact on the battery and the bidirectional DC-DC converter. On the contrary, ACO-PSO proved its excellent speed adaptability by providing a quicker and smoother current response. Although both algorithms had managed to regulate the current, GA had exhibited significantly higher oscillations compared to ACO-PSO. These kinds of fluctuations might have damaged the battery as well as the bidirectional DC-DC converter, which suggests that GA was not very dependable in terms of current regulation. On the other hand, ACO-PSO was giving a faster and smoother current response, thus pointing out its excellence in adaptation under ever-changing speed conditions. The dynamic armature voltage response that can be seen in Figure 16 demonstrated the direct relationship with the reference speed; the higher speeds were accompanied by higher voltage levels, and the lower speeds by diminished voltage. The ACO-PSO algorithm not only managed to suppress voltage oscillations better but also reached the changes in reference speed faster. On the downside, it was producing somewhat larger ripples than GA. Nevertheless, this tiny drawback did not affect ACO-PSO's quick adaptation and overall voltage stability, which was even better than GA's during speed fluctuations and mode shifts.

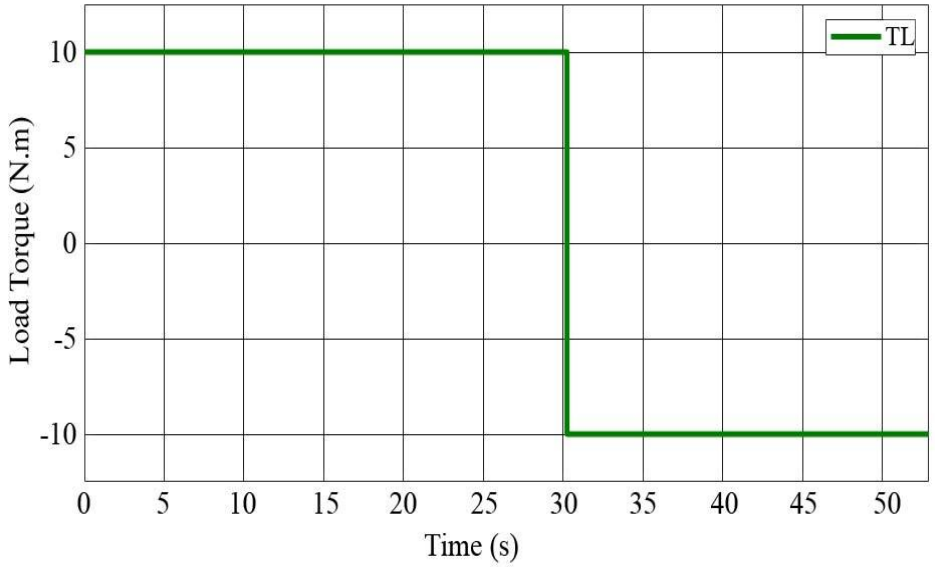

Fig. 13 Load Torque

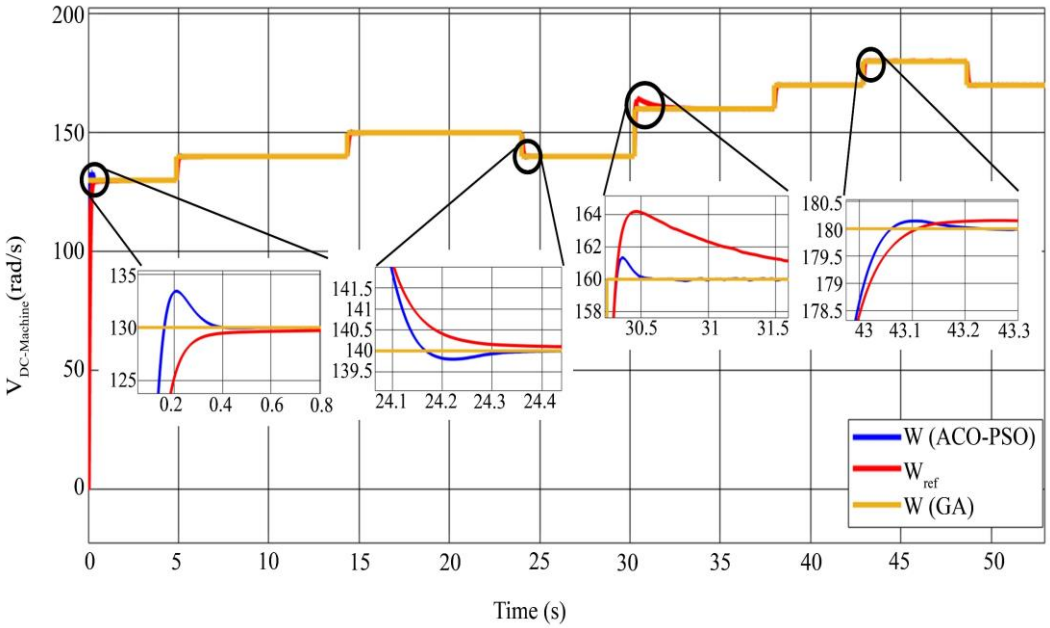

Fig. 14 Dynamic DC machine speed variation

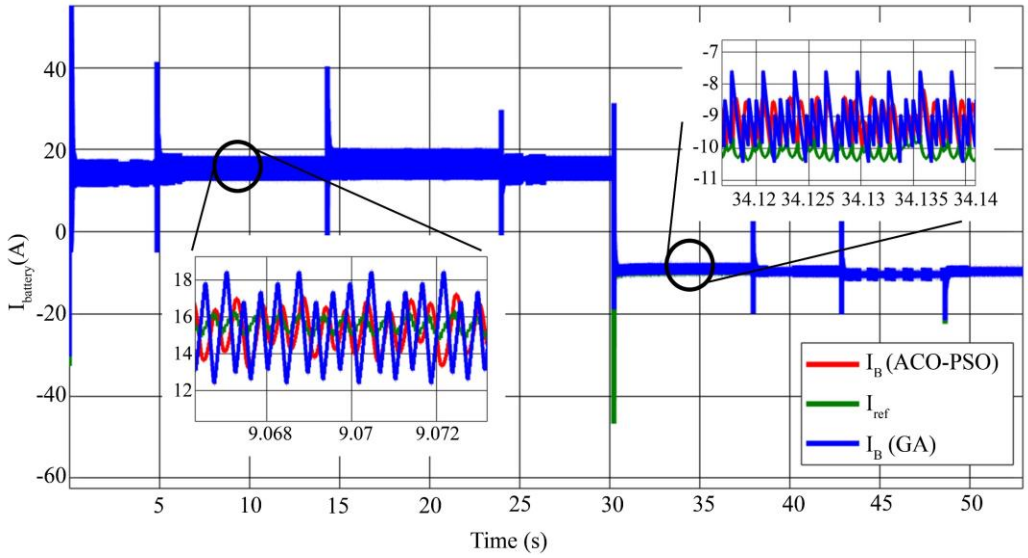

Fig. 15 Dynamic battery current variation

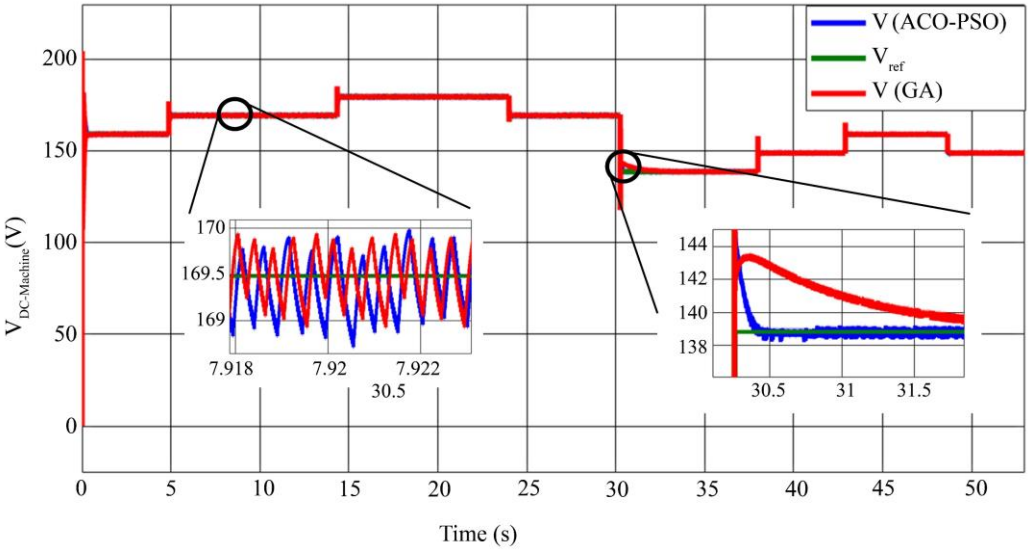

Fig. 16 Dynamic armature voltage variation

5. Conclusion

This work presented a comparative study on the evolutionary tuning of cascaded PI controllers for DC machine speed control in Meca-Electrical Wind Pumping Systems. Two optimization methods, GA and ACO-PSO, were adopted and assessed with the help of cost function convergence, PI parameter adaptation, and dynamic performance indices.

The results indicated that ACO-PSO was superior to GA at all times regarding convergence speed, overshoot reduction, and reliability under sudden disturbances. In the first scenario (constant speed variable load torque), ACO-PSO quickly stabilized with minor overshoot, whereas GA was heavily oscillated and slowly recovered. In a similar manner, in the second scenario (constant torque with variable speed), ACO-PSO was faster than GA during the transitions; it settled in 0.5 seconds, while GA took 3 seconds before it was completely stable. Even though ACO-PSO caused a bit more voltage ripple in dynamic armature voltage, it still displayed better overall performance in current regulation, voltage stability, and dynamic speed tracking, which led to its acceptance for MEWPS applications. Such results encourage the use of hybrid optimization methods as a means of ensuring the reliability and efficiency of control systems for the stable operation of renewable-driven water pumping systems. Future work can build on the current study by carrying out the proposed controller in real time, exploring multi-objective optimization in order to find the proper trade-off between energy efficiency and reliability, and integrating cutting-edge control strategies such as Sliding Mode Control, Model Predictive Control, etc., for superior efficiency in variable wind conditions.

References

[1] Patrick Thomson, "Remote Monitoring of Rural Water Systems: A Pathway to Improved Performance and Sustainability?," *WIREs Water*, vol. 8, no 2, pp. 1-14, 2021. [CrossRef] [Google Scholar] [Publisher Link]

[2] Andrea I. Schäfer, Gordon Hughes, and Bryce S. Richards, "Renewable Energy Powered Membrane Technology: A Leapfrog Approach to Rural Water Treatment in Developing Countries," *Renewable and Sustainable Energy Reviews*, vol. 40, pp. 542-556, 2014. [CrossRef] [Google Scholar] [Publisher Link]

[3] Ehsan Elahi, Zainab Khalid, and Zhixin Zhang, "Understanding Farmers' Intention and Willingness to Install Renewable Energy Technology: A Solution to Reduce the Environmental Emissions of Agriculture," *Applied Energy*, vol. 309, 2022. [CrossRef] [Google Scholar] [Publisher Link]

[4] Sachin Angadi et al., "Comprehensive Review on Solar, Wind and Hybrid Wind-PV Water Pumping Systems-An Electrical Engineering Perspective," *CPSS Transactions on Power Electronics and Applications*, vol. 6, no. 1, pp. 1-19, 2021. [CrossRef] [Google Scholar] [Publisher Link]

[5] Sakon Klongboonjit, and Tossapol Kiatcharoenpol, "Priority of Wind Energy in West Coast of Southern Thailand for Installing the Water Pumping Windmill System with Combining of Entropy Weight Method and TOPSIS," *Energies*, vol. 16, no. 20, pp. 1-13, 2023. [CrossRef] [Google Scholar] [Publisher Link]

[6] Muhammad Zeeshan Abid et al., "Design, Sizing and Economic Feasibility of a Hybrid PV/Diesel/Battery-Based Water Pumping System for Farmland," *International Journal of Green Energy*, vol.19, no. 6, pp. 614-637, 2022. [CrossRef] [Google Scholar] [Publisher Link]

[7] Muhammad Hilal Mthboob, Haider TH. Salim ALRikabi, and Ibtisam A. Aljazaery, "A Concepts and Techniques Related to the DC Motor Speed Control System Design: Systematic Review," *Wasit Journal of Computer and Mathematics Science*, vol. 2, no. 1, pp. 59-73, 2023. [CrossRef] [Google Scholar] [Publisher Link]

[8] Ikram Saady et al., "Improving Photovoltaic Water Pumping System Performance with ANN-Based Direct Torque Control using Real-Time Simulation," *Scientific Reports*, vol. 15, no. 1, pp. 1-28, 2025. [CrossRef] [Google Scholar] [Publisher Link]

[9] Zhenlong Wu et al., "Optimized Cascaded PI Controller for the Load Frequency Regulation of Multi-Area Power Systems with Communication Delays," *Energy Reports*, vol. 8, no. Sup13, pp. 469-477, 2022. [CrossRef] [Google Scholar] [Publisher Link]

[10] Anurag Savarn, Vimlesh Verma, and Md. Nishat Anwar, "Design of Direct Synthesis-Based Cascaded PI Controller for PMSM Drive with Improved Nonlinear Disturbance Observer," *International Journal of Circuit Theory and Applications*, 2025. [CrossRef] [Google Scholar] [Publisher Link]

[11] Sai Zhang et al., "Comparative Study of Several PID Parameter Tuning Methods," *Tenth International Conference on Mechanical Engineering, Materials, and Automation Technology*, Wuhan, China, 2024. [CrossRef] [Google Scholar] [Publisher Link]

[12] Laith Abualigah et al., "Meta-Heuristic Optimization Algorithms for Solving Real-World Mechanical Engineering Design Problems: A Comprehensive Survey, Applications, Comparative Analysis, and Results," *Neural Computing and Applications*, vol. 34, no. 6, pp. 4081-4110, 2022. [CrossRef] [Google Scholar] [Publisher Link]

[13] Qifan Yang, and Ningyi Dai, "Genetic Algorithm for PI Controller Design of Grid-Connected Inverter based on Multilayer Perceptron Model," *2021 IEEE Sustainable Power and Energy Conference (iSPEC)*, Nanjing, China, pp. 2770-2775, 2021. [CrossRef] [Google Scholar] [Publisher Link]

[14] Rahul Priyadarshi, and Ravi Ranjan Kumar, "Evolution of Swarm Intelligence: A Systematic Review of Particle Swarm and Ant Colony Optimization Approaches in Modern Research," *Archives of Computational Methods in Engineering*, vol. 32, no. 6, pp. 3609-3650, 2025. [CrossRef] [Google Scholar] [Publisher Link]

[15] Sisir Kumar Yadav, Ashish Patel, and Hitesh Datt Mathur, "A Novel Particle Swarm Optimization-Based Plant-in-Loop Tuning Method for PI Controller of Integrated Power Converters," *IEEE Journal of Emerging and Selected Topics in Power Electronics*, vol. 13, no. 3, pp. 3756-3765, 2025. [CrossRef] [Google Scholar] [Publisher Link]

[16] Abd. Harris Hamma, Salama Manjang, and Ikhlas Kitta, "Implementation of Ant Colony Optimization and Particle Swarm Optimization for Power Plant Operation Optimization," *2025 4th International Conference on Electronics Representation and Algorithm (ICERA)*, Yogyakarta, Indonesia, pp. 12-17, 2025. [CrossRef] [Google Scholar] [Publisher Link]

[17] Kapil Choudhary, *Ant Colony Optimization-Based Models for Agriculture Price Forecasting: Innovations, Case Studies, and Future Prospects*, IntechOpen, 2024. [CrossRef] [Google Scholar] [Publisher Link]

[18] Gudur Balawanth Reddy, Gautam Poddar, and Bishnu Prasad Muni, "Parameter Estimation and Online Adaptation of Rotor Time Constant for Induction Motor Drive," *IEEE Transactions on Industry Applications*, vol. 58, no. 2, pp. 1416-1428, 2022. [CrossRef] [Google Scholar] [Publisher Link]

[19] Senthil Kumar Ramu et al., "Enhanced Energy Management of DC Microgrid: Artificial Neural Networks-Driven Hybrid Energy Storage System with Integration of Bidirectional DC-DC Converter," *Journal of Energy Storage*, vol. 88, 2024. [CrossRef] [Google Scholar] [Publisher Link]

[20] G. Sugumaran, and N. Amutha Prabha, "A Comprehensive Review of Various Topologies and Control Techniques for DC-DC Converter-Based Lithium-Ion Battery Charge Equalization," *International Transactions on Electrical Energy Systems*, vol. 2023, no. 1, pp. 1-21, 2023. [CrossRef] [Google Scholar] [Publisher Link]

[21] Zhila Yaseen Taha, Abdulhady Abas Abdullah, and Tarik A. Rashid, "Optimizing Feature Selection with Genetic Algorithms: A Review of Methods and Applications," *Knowledge and Information Systems*, vol. 67, no.11, pp. 9739-9778, 2025. [CrossRef] [Google Scholar] [Publisher Link]

[22] Jinrui Gao et al., "Particle Swarm Optimization with Problem-Aware Hyperparameter Design for Feature Selection in High Dimensions," *Information Sciences*, vol. 722, 2025. [CrossRef] [Google Scholar] [Publisher Link]

[23] R. Satheeshkumar et al., "Frequency Management of an Interconnected Power System using Ant Colony Optimization Technique Enhanced PI Controller," *Proceedings of International Conference on Data Analytics and Insights*, Kolkata, India, pp. 505-514, 2023. [CrossRef] [Google Scholar] [Publisher Link]